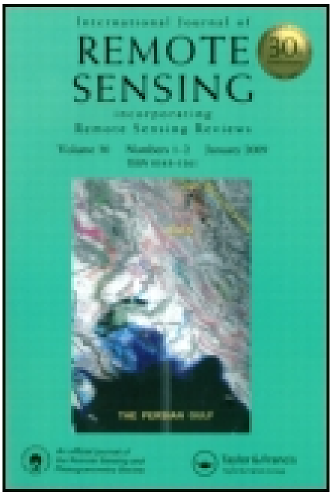

International Journal of Remote Sensing
Publication details, including instructions for authors and subscription information:
http://www.tandfonline.com/loi/tres20

Instrumentation complex for comprehensive study of atmospheric parameters

G.G. Matvienko[a], B.D. Belan[a], M.V. Panchenko[a], S.M. Sakerin[a], D.M. Kabanov[a], S.A. Turchinovich[a], Yu.S. Turchinovich[a], T.A. Eremina[a], V.S. Kozlov[a], S.A. Terpugova[a], V.V. Pol'kin[a], E.P. Yausheva[a], D.G. Chernov[a], S.L. Odintsov[a], V.D. Burlakov[a], M.Yu. Arshinov[a], G.A. Ivlev[a], D.E. Savkin[a], A.V. Fofonov[a], V.A. Gladkikh[a], A.P. Kamardin[a], D.B. Belan[a], M.V. Grishaev[a], V.V. Belov[a], S.V. Afonin[a], Yu.S. Balin[a], G.P. Kokhanenko[a], I.E. Penner[a], S.V. Samoilova[a], P.N. Antokhin[a], V.G. Arshinova[a], D.K. Davydov[a], A.V. Kozlov[a], D.A. Pestunov[a], T.M. Rasskazchikova[a], D.V. Simonenkov[a], T.K. Sklyadneva[a], G.N. Tolmachev[a], S.B. Belan[a], V.P. Shmargunov[a], B.A. Voronin[a], V.I. Serdyukov[a], E.R. Polovtseva[a], S.S. Vasil'chenko[a], O.V. Tikhomirova[a], Yu.N. Ponomarev[a], O.A. Romanovskii[ab], L.N. Sinitsa[ab], V.N. Marichev[a], M.V. Makarova[c], A.S. Safatov[d], A.S. Kozlov[e], S.B. Malyshkin[e] & T.A. Maksimova[e]

[a] V.E. Zuev Institute of Atmospheric Optics SB RAS, 634021 Tomsk, Russia

[b] National Research Tomsk State University, 634050 Tomsk, Russia

[c] Saint Petersburg State University, 198504 Saint Petersburg, Russia

[d] State Research Centre of Virology and Biotechnology, 'Vektor', 630559 Koltsovo, Novosibirsk reg., Russia

[e] Voevodsky Institute of Chemical Kinetics and Combustion SB RAS, 630090 Novosibirsk, Russia

Published online: 28 Aug 2014.

International Journal of Remote Sensing, 2014
Vol. 35, No. 15, 5651–5676, http://dx.doi.org/10.1080/01431161.2014.945015

Instrumentation complex for comprehensive study of atmospheric parameters

G.G. Matvienko[a], B.D. Belan[a], M.V. Panchenko[a], S.M. Sakerin[a], D.M. Kabanov[a], S.A. Turchinovich[a], Yu.S. Turchinovich[a], T.A. Eremina[a], V.S. Kozlov[a], S.A. Terpugova[a], V.V. Pol'kin[a], E.P. Yausheva[a], D.G. Chernov[a], S.L. Odintsov[a], V.D. Burlakov[a], M.Yu. Arshinov[a], G.A. Ivlev[a], D.E. Savkin[a], A.V. Fofonov[a], V.A. Gladkikh[a], A.P. Kamardin[a], D.B. Belan[a], M.V. Grishaev[a†], V.V. Belov[a], S.V. Afonin[a†], Yu.S. Balin[a], G.P. Kokhanenko[a], I.E. Penner[a], S.V. Samoilova[a], P.N. Antokhin[a], V.G. Arshinova[a], D.K. Davydov[a], A.V. Kozlov[a], D.A. Pestunov[a], T.M. Rasskazchikova[a], D.V. Simonenkov[a], T.K. Sklyadneva[a], G.N. Tolmachev[a], S.B. Belan[a], V.P. Shmargunov[a], B.A. Voronin[a]*, V.I. Serdyukov[a], E.R. Polovtseva[a], S.S. Vasil'chenko[a], O.V. Tikhomirova[a], Yu.N. Ponomarev[a], O.A. Romanovskii[a,b], L.N. Sinitsa[a,b], V.N. Marichev[a], M.V. Makarova[c], A.S. Safatov[d], A.S. Kozlov[e], S.B. Malyshkin[e], and T.A. Maksimova[e]

[a]*V.E. Zuev Institute of Atmospheric Optics SB RAS, 634021 Tomsk, Russia;* [b]*National Research Tomsk State University, 634050 Tomsk, Russia;* [c]*Saint Petersburg State University, 198504 Saint Petersburg, Russia;* [d]*State Research Centre of Virology and Biotechnology, 'Vektor', 630559 Koltsovo, Novosibirsk reg., Russia;* [e]*Voevodsky Institute of Chemical Kinetics and Combustion SB RAS, 630090 Novosibirsk, Russia*

(*Received 3 July 2013; accepted 17 March 2014*)

A unique instrumentation complex of the Institute of Atmospheric Optics SB RAS is presented. The complex has no analogues anywhere in the world, and makes possible simultaneous measurements of a great number of optical, meteorological, and radiative parameters of the atmosphere, as well as characteristics of aerosol and gas composition. The instrumentation complex is based on permanent stations recording numerous parameters of the atmosphere, namely, TOR (Tropospheric Ozone Research) station, Aerosol Monitoring Station, BEC (Basic Experimental Complex), Fonovaya (Background) Station, and stations for receiving satellite images (NOAA, MODIS/TERRA, MODIS/AQUA). An important part of the complex is the Tu-134 aircraft laboratory enabling measurement of atmospheric parameters in the altitude range up to 7 km. In addition, the following instruments are used in experiments: weather balloons, lidars, sodars, sun photometers, Fourier spectrometers, and others. Satellite data are also used for interpretation of data. The article presents an example of complex operation on one measurement day – 22 May 2012.

1. Introduction

Climate change observed for more than one decade is recognized by the entire global community, and numerous national and international programmes are devoted to the investigation of possible causes and prediction of further climatic tendencies. Despite the common recognition of this problem, there is no consensus on the role of human

*Corresponding author. Email: vba@iao.ru
†Deceased

activity in global climate change. Thus, the studies of Antarctic ice cores have shown that over the last 650,000 years there were several periods of global warming (Solomon et al. 2007) accompanied by an increase in the concentration of major greenhouse gases (CO_2, CH_4, and N_2O). It was found that the increase of temperature in the Antarctic region started several centuries before the increase in CO_2 concentration (Monnin et al. 2001).

Although the important role of aerosols in climate change is well established, the level of understanding of the indirect effect of aerosol in radiative changes remains very low. This fact complicates significantly the prediction of global changes in the Earth's climate.

The permanent development and improvement of climatic models requires an increasingly greater amount of data from field measurements conducted in different regions of the world. The territory of Siberia, occupying about 10% of the world's land area, has practically no cover by the modern observation network. Meanwhile, Siberia lies within several climatic zones, its ecosystems are very various, and therefore the intensity of sources and sinks of atmospheric admixtures are likely to vary significantly.

Taking into account that each of the methods applied for the investigation of aerosol characteristics is informative only in a certain wavelength range, only the combined analysis of all available experimental data can provide the correct reconstruction of the complete optical pattern of tropospheric aerosol in a particular region.

The objective of this study was to conduct simultaneous measurements of microphysical, chemical, and optical properties of aerosol particles in the atmospheric surface layer and in the free atmosphere with our unique set of ground-based, airborne, and spaceborne instruments, in order to create a complete pattern of the composition and state of the atmosphere over the territory of Western Siberia.

In this connection, the following tasks were set:

- modernization and intercalibration of developed measurement tools;
- conduction of measurement cycles;
- reconstruction of the whole set of microphysical, chemical, and optical characteristics of aerosol from experimental findings;
- study and analysis of the influence of vertical variability of optical characteristics of tropospheric aerosol on radiative effects of aerosol under typical conditions in Western Siberia

.

2. Measurement system

The measurement system developed provides sun-photometric measurements of the aerosol optical depth of the atmosphere, acoustic sounding of the boundary layer, laser sensing of the aerosol content in the troposphere and stratosphere, measurement of the gas composition of the atmosphere (including greenhouse gases), and measurement of meteorological parameters of air, in particular, with weather balloons.

The composition and purpose of individual elements of the measurement system are summarized in Table 1.

We first consider the systems used for measurement in surface air and then describe the devices for determination of the integral content of desired parameters and their vertical distributions.

Continuous measurement of the concentration of minor atmospheric constituents was carried out at three stations for monitoring of atmospheric composition relating to IAO SB RAS (Figure 5): Fonovaya Observatory, TOR (Tropospheric Ozone Research) station, and Basic Experimental Complex (BEC).

Table 1. Composition and purpose of individual elements of the measurement system.

No.	Element	Produced by	Measurements since	Purpose	URL
1	TOR (Tropospheric Ozone Research) station	IAO SB RAS, RUSSIA	1992	Monitoring of meteorological parameters, gas and aerosol composition of air, and solar radiation in the surface layer	http://lop.iao.ru/eng/index.php/about–tor–station/aero–tor
2	Basic Experimental complex	IAO SB RAS, RUSSIA	1986	Monitoring of meteorological parameters, gas and aerosol composition of air, and solar radiation in the surface layer	http://lop.iao.ru/eng/index.php/about–bec/aerosols
3	Fonovaya (Background) Station	IAO SB RAS, RUSSIA	1978	Monitoring of meteorological parameters, gas and aerosol composition of air, and solar radiation in the surface layer	http://lop.iao.ru/eng/index.php/about–fonovyi/aerosols–2
4	Ty–134 Optik aircraft–laboratory	IAO SB RAS, RUSSIA	1988	Measurement of meteorological parameters, gas and aerosol composition of air, optical characteristics of air	http://www.iao.ru/en/resources/equip/plane/
5	DigiCora 3 system for radiosounding of the atmosphere	Vaisala Oy, Finland	2006	Determination of vertical distribution of meteorological parameters by contact tools	http://www.vaisala.ru/Vaisala%20Documents/Brochures%20and%20Datasheets/RS92SGP–Datasheet–B210358RU–E–LoRes.pdf
6	SP–9 sun photometer	IAO SB RAS, RUSSIA	2010	Measurement of aerosol optical thickness and water column of the atmosphere	http://link.springer.com/article/10.1134/S102485601304012X
7	Aerosol Station	IAO SB RAS, RUSSIA	1996	Measurement of characteristics of surface aerosol	http://aerosol1.iao.ru/index.php?lang=eng
8	LOZA lidar	IAO SB RAS, RUSSIA	1992	Determination of aerosol profile at a distance of 1–10 km in any direction of the hemisphere	http://www.iao.ru/en/resources/equip/lidars/loza/
9	2.4 XLB direct broadcast reception system	Orbital Systems, USA	2011	Reception of satellite data from AVHRR, MODIS, and other optoelectronic devices	http://www.orbitalsystems.com/antenna–products/systems/eosdb–systems/
10	Meteo–2 Ultrasonic meteostation	IAO SB RAS, RUSSIA	2007	Measurement of mean values and characteristics of wind turbulence and air temperature	http://www.iao.ru/en/resources/equip/dev/meteo2/

(*Continued*)

Table 1. (*Continued*).

No.	Element	Produced by	Measurements since	Purpose	URL
11	Volna Sodar	IAO SB RAS, RUSSIA	2006	Measurement of vertical profiles of wind vector components in the atmospheric boundary layer	http://www.iao.ru/en/resources/equip/dev/sodar/
12	Siberian Lidar Station	IAO SB RAS, RUSSIA	1988	High-altitude sensing of the atmosphere	http://www.iao.ru/en/resources/equip/sls/
13	Lidar station for altitude sounding of the atmosphere	IAO SB RAS, RUSSIA	1986	Observation of the vertical stratification of aerosol ozone concentration and temperature in the stratosphere and mesosphere	http://link.springer.com/article/10.3103/S1068373911090056
14	Sun tracker based on IFS–125M Fourier spectrometer	IAO SB RAS, RUSSIA	2010	Measurement of gas constituents of the atmosphere	http://link.springer.com/article/10.1134/S1024856013030147

The measured parameters are summarized in Table 2, and the operation of all the stations is described in detail by Arshinov et al. (2007).

For the monitoring of measurements and the state of the systems, information from each station is collected every hour through transfer of all parameters to a central server. As a result, the state of the atmosphere is monitored in the virtual online mode. The graphic presentation of the monitored parameters is available at http://lop.iao.ru/activity/?id=mes, which is updated every one hour. The interface allows the selection of different options for viewing the current information both separately for each station and for a particular parameter measured at all the three stations.

To study the vertical distribution of the climatically significant components of the troposphere, we used the analytical equipment (Figure 1) installed on board the Optik Tu-134 flying laboratory (Anokhin et al. 2011).

Since the main purpose of our experiment was to study the radiative characteristics of the atmosphere, below we describe the equipment used to measure atmospheric admixtures as major contributors to radiative forcing.

To study the vertical distribution of the main greenhouse gases, we used the Picarro G2301-m precision gas analyser specially designed for onboard use, which allows the simultaneous measurement of carbon dioxide, methane, and water vapour concentrations with a frequency of 1 Hz (http://www.picarro.com/gas_analyzers/flight_co2_ch4_h2o). The operating principle of the gas analyser is based on the cavity ringdown spectroscopy method, which allows determination of the spectral characteristics of gas molecules in an optical cavity. Now this device is the best available, since the accuracy of measurement of CO_2, CH_4, and H_2O concentrations is <200 ppb, <1.5 ppb, and <150 ppm, respectively.

The ozone concentration was measured with the TEI Model 49C UV photometric gas analyser modified for measurements from aircraft of different types (Marenco et al. 1998). The accuracy of measurement of O_3 concentration was 1 ppb at an integration time of 4 s.

The vertical structure of the distribution of atmospheric aerosols was reconstructed with the use of two types of device. The first type includes the diffusion aerosol spectrometer (DAS), which allows the number distribution of nanoaerosols to be reconstructed in the size range from 3 to 200 nm in 20 size intervals. DAS consists of an eight-channel mesh-type diffusion battery (DB) and a condensation particle counter. The principle of particle separation by size is based on the size dependence of the diffusion coefficients of nanoparticles. As a result, particles of different size passing through porous media have different deposition rates: smaller particles leave the flow more quickly, and thus the coefficient of particle passage through such a medium carries the information about particle size. Particle concentration is measured after each DB channel with the WCPC 3781 condensation particle counter (TSI Inc., Shoreview, MN, USA). After every scan of all DB channels, the size spectrum is reconstructed using the algorithm developed by Eremenko and Ankilov (1995) with regard to WCPC 3781's counting efficiency. Due to the use of the WCPC 3781 condensation particle counter with a response time <2 s, the full-size distribution of nanoparticles was obtained in 80 s.

The second type includes the Grimm #1.109 laser aerosol spectrometer (Grimm Aerosol Technik GmbH & Co., Ainring, Germany), used for the measurement of aerosol particle number density in 31 size intervals: 0.25, 0.28, 0.3, 0.35, 0.4, 0.45, 0.5, 0.58, 0.65, 0.7, 0.8, 1.0, 1.3, 1.6, 2, 2.5, 3, 3.5, 4, 5, 6.5, 7.5, 8.5, 10, 12.5, 15, 17.5, 20, 25, 30, and 32 μm. The operating principle of this spectrometer is based on the dependence of the scattered radiation intensity on particle size. At a known air-flow rate, the pulse repetition frequency allows the concentration of particles in the air to be determined.

Table 2. Measurement facilities and their characteristics.

Unit	Device/sensor	Parameter	Range	Error	Time constant
		TOR Station			
Weather station	HIH-3602-C	t (°C)	–40…+85	±0.1°C	1 s
	HIH-3602-C	U (%)	0…100	±2%	1 s
	M-63	dd (°)	0…360	±10°	1 s
	M-63	V (m s^{-1})	1.2…40	±(0.5 + 0.05V)	1 s
	MPX4115AP	P (hPa)	150…1150	±1.5	0.001 s
Gas analyser	G2301-m	CO_2 (ppm)	0…1000	<0.2 ppm	1 s
		CH_4 (ppm)	0…20	<0.0015 ppm	1 s
		H_2O (ppm)	0…70000	<150 ppm	1 s
	3.02-P	O_3 (μg m^{-3})	0…500	±20%	1 s
	R-310	NO/NO_2 (μg m^{-3})	0…1000	±25%	160 s
	K-100	CO (mg m^{-3})	0…50	±20%	1 s
	API 100E	SO_2 (ppm)	0…20	±0.5%	20 s
	Brewer 049	TOC (D.u.)	–	±1%	120 s
Aerosol system	GRIMM #1.109	D_p (μm) (31 channels)	0.25…32	–	6 s
		N (cm^{-3})	0…2000	±3%	
	Diffusional aerosol spectrometer	D_p (nm) (20 channels)	3…200	–	80 s
		N (cm^{-3})	0…500000	±10%	
Air ions	Sapphire-3M	N (cm^{-3})	0…2500,000	±5%	4 s
Radiation unit	M-115	λ (μm)	0.3…2.4	±10%	<40 s
		Q (W m^{-2})	0…1500		
	YES UVB-1	λ (nm)	280…320	–	0.1 s
		I (W m^{-2})	0…2.5	<5%	
	Brewer 049	λ (nm)	290…325	–	265 s
		I (W m^{-2})	–	–	
Gamma background	IRF	γ–background (μR h^{-1})	1…1000	30%	1 s
		BEC			
Weather station	HIH-3602-C	t (°C)	–40… + 85	±0.1°C	1 s
	HIH-3602-C	U (%)	0…100	±2%	1 s
	M-63	dd (°)	0…360	±10°	1 s
	M-63	V (m s^{-1})	1.2…40	±(0.5 + 0.05V)	1 s
	MPX4115AP	P (hPa)	150…1150	±1.5	0.001 s

(*Continued*)

Table 2. (*Continued*).

Unit	Device/sensor	Parameter	Range	Error	Time constant
Gas analyser	LI-820	CO_2 (ppm)	0…1000	<0.2* ppm	1 s
	3.02-P	O_3 (μg m^{-3})	0…500	±20%	1 s
	API 200E	NO/NO_2 (ppm)	0…20	±0.5%	20 s
	K-100	CO (mg m^{-3})	0…50	±20%	1 s
	ME 9850B	SO_2 (ppm)	0…20	±1%	<20 s
	HCNM 2000G	CH_4 and ΣCH (ppm)	0…10	0.1	120 s
Aerosol system	GRIMM #1.108	D_p (μm) (15 channels)	0.3…20	–	6 s
		N (cm^{-3})	0…2000	±3%	
		Fonovaya Observatory			
Weather station	HIH-3602-C	t (°C)	–40… + 85	±0.1°C	1 s
	HIH-3602-C	U (%)	0…100	±2%	1 s
	M-63	dd (°)	0…360	±10°	1 s
	M-63	V (m s^{-1})	1.2…40	±(0.5 + 0.05V)	1 s
	MPX4115AP	P (hPa)	150…1150	±1.5	0.001 s
Gas analyser	FGGAModel 907-0010	CO_2 (ppm)	20…10000	0.2 ppm	1 s
		CH_4 (ppm)	0.005…50	0.001 ppm	
		H_2O (ppm)	150…70000	100 ppm	
	LI-840	CO_2 (ppm)	0…1000	<0.2* ppm	1 s
	3.02-P	O_3 (μg m^{-3})	0…500	±20%	1 s
	R-310	NO/NO_2 (μg m^{-3})	0…1000	±25%	160 s
	K-100	CO (mg m^{-3})	0…50	±20%	1 s
	S-310	SO_2 (mg m^{-3})	0…2	±25%	142 s
Aerosol system	GRIMM #1.108	D_p (μm) (15 channels)	0.3…20	–	6 s
		N (cm^{-3})	0…2000	±3%	
	Diffusional aerosol spectrometer	D_p (nm) (20 channels)	3…200	–	160 s
		N (cm^{-3})	0…1000000	±10%	
Air ions	Sapphirer-3M	N (cm^{-3})	0…2500000	±5%	4 s

Note: * at calibration against standard gas mixtures

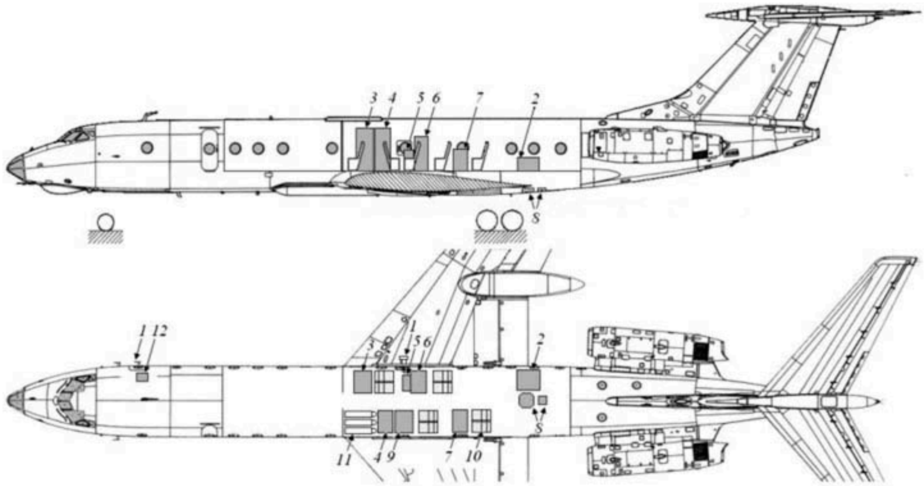

Figure 1. Arrangement of scientific equipment on board the Optik Tu–134 flying laboratory: *1* – air intakes; *2* – power supply unit for airborne equipment; *3* – instrument rack for the gas analysers: O_3 (TEI (Thermo Environmental Instruments) Model 49C), SO_2 (T–API 100E), and DAS (diffusion aerosol spectrometer); *4* – instrument rack for the gas analysers: CO_2 (CONDOR), $CO_2/CH_4/H_2O$ (Picarro G2301–m), O_3 (TEI Model 49C), and CO (TEI Model 48C); *5* – rack for the filter–aspiration setup, laser aerosol spectrometer (Grimm Model 1.109), and O_3 gas analyser (OPTEK 3.02P); *6* – instrument rack for aethalometer and flow-through nephelometer (FAN); *7* – rack for the central onboard computer; *8* – camera windows; *9* – instrument rack for the CO_2 gas analyser (LI–6262) and portal of air sampling into flasks; *10* – operator chairs; *11* – span gas cylinders; *12* – device for sampling onto filters for analysis of the organic component of aerosol.

Thus, in combination, these two spectrometers form an aerosol system covering the size range from 3 nm to 32 μm with good resolution.

Temperature–wind sounding was carried out with the Vaisala DigiCORA® MW31 radiosonde (Vaisala R92SGP, http://www.vaisala.ru). The combination of this radiosonde and GPS correlator with the DigiCORA® system provides the optimal level of measurement of atmospheric pressure (*P*), temperature (*t*), and relative air humidity (*U*), as well as permanent wind data.

Several types of sun photometer are used in measurements of aerosol optical thickness (AOT) and atmospheric water content. In 2012, two devices were used:

(1) SP-9 multiwave sun photometer for regular measurement of AOT in the spectral range 0.34–2.14 μm (16 spectral channels) and atmospheric water content, as well as for reconstruction of aerosol microstructural parameters (Sakerin et al. 2004, 2012);
(2) CIMEL CE 318 Sun-Sky radiometer of the AERONET global network for determination of AOT in the spectral range 0.34–1.02 μm, water content *W*, asymmetry factor of aerosol backscattering phase functions, aerosol single scattering albedo, microstructural parameters of particles sized from 0.1 to 10 μm, and others (Holben et al. 1998; Dubovik and King 2000; Dubovik et al. 1998, 2000).

Aerosol measurements at the stationary IAO SB RAS Aerosol Station (Kozlov et al. 1997, 2002) are conducted using the methods for investigation of aerosol properties in local air volumes, that is, air with aerosol is pumped through optical cells (flow-through measurements). The surface aerosol reaches optical cells by ducts through air intakes installed outside the main building of IAO SB RAS at a height of 9 m above the surface.

The aerosol measurement system includes such devices as angle-scattering nephelometers (Kozlov et al. 2002; Shmargunov et al. 2008), photoelectric particle counters from scattered radiation (Shmargunov and Pol'kin 2007), and aethalometers (Kozlov et al. 2002; Kozlov, Panchenko, and Yausheva 2008), that is, devices measuring the characteristics of aerosol absorption. The FAN-type angular nephelometer provides the measurement of directed aerosol scattering coefficient at an angle of 45° at a wavelength of 0.51 μm, which is proportional to the concentration of submicron aerosol (Kozlov, Shmargunov, and Pol'kin 2008). The nephelometer allows the directed scattering coefficient to be measured starting from the level of molecular scattering ~1 mm^{-1} $ster^{-1}$. The nephelometer has been calibrated under laboratory conditions against the known value of molecular scattering of radiation by pure air at the pumpdown pressure in the nephelometer cell from 760 to 350 mm Hg. To measure characteristics of the dispersed composition of aerosol particles, the modified PKGTA photoelectric particle counter (particle diameter 0.4–10 μm) is used (Shmargunov and Pol'kin 2007).

The mass concentration of black carbon in the composition of aerosol particles is measured with an MDA three-wave differential aethalometer developed in IAO SB RAS (Sakerin et al. 2004). The concentration sensitivity of the aethalometer when 30 l of air is pumped through is about 10 ng m^{-3}. The aethalometer has been calibrated under laboratory conditions with the aid of a pyrolysis generator of soot (black carbon) particles and the comparison of data of synchronous optical and gravimetric measurements.

The aureole photometer measures the directed scattering coefficient in an angular range of 1.2–20° and is used for estimation of the mass content of coarse particles in the size spectrum (Shmargunov et al. 2010).

The system of active polarization nephelometry, which is also used at the Aerosol Station, includes the FAN nephelometer and devices for artificial humidification of aerosol up to 90% relative humidity of air or for heating up to 250°C. It serves for the measurement of aerosol hygro- and thermograms, which are used for determination of the parameter of hygroscopic activity of particles and the fractional content of volatile compounds in aerosol. Polarization measurements with this system allow the microstructure and optical constants of submicron aerosol particles to be determined through solution of the inverse problem.

Remote laser sensing of aerosol fields in the vertical depth of the troposphere was carried out with the stationary multifrequency LOZA lidar at three laser wavelengths of 355, 532, and 1064 nm, with a laser pulse repetition frequency of 20 Hz and pulse duration of 10 ns. The lidar system detects not only echo signals of elastic backscattering, but also signals of Raman scattering by molecular nitrogen (387 and 607 nm) and water vapour (407 nm) at the same wavelengths at night-time. Polarization components of backscattered radiation at a wavelength of 532 nm were measured in an additional channel. The multifrequency lidar provides reconstruction of high-quality information about the vertical (from the surface to the lower stratosphere) distribution of optical (scattering and extinction coefficients, optical depth) and microphysical (nonsphericity, phase composition, mean size spectrum of aerosol particles within the identified layer) properties of aerosol. For more detailed description of the lidar and the methods for reconstruction of optical parameters, see Samoilova et al. (2009).

For monitoring of temperature, humidity, ozone, aerosol, and clouds with a spatial resolution of 1–10 km, the data of the MODIS multichannel spectroradiometer (spectral range of 0.4–14 μm) installed on the Terra and Aqua platforms of the EOS satellite system were mostly used.

The sounding of minor gas constituents (MGCs) from space was carried out with a spectral resolution of 0.35–0.5 cm^{-1} in the range 645–2760 cm^{-1} with the Infrared Atmospheric Sounding Interferometer (IASI) Fourier spectrometer from the MetOP-A satellite and with a spatial resolution of 25–100 km depending on MGC. In addition to the IASI data, data of the Atmospheric Infrared Sounder (AIS) from the Aqua satellite with the nominal spatial resolution of ~45 km and spectral resolution $\lambda/\Delta\lambda$ ~1200 in 2378 channels lying in the ranges 3.74–4.61, 6.20–8.22, and 8.80–15.40 μm were used for the same purposes. Information about satellite dishes can be found at http://www.orbitalsystems.com/antenna-products/systems/eosdb-systems.

The measurement system includes facilities for local and remote acoustic diagnostics of the atmospheric boundary layer, namely, Meteo-2 Ultrasonic Meteostations (UMSs) (Gladkikh and Makienko 2009) and Volna-4 three-channel acoustic Doppler sodar, whose main operating principles and some results are described in Gladkikh, Kamardin, and Nevzorova (2009); Odintsov and Fedorov (2007); and Gladkikh, Makienko, and Fedorov (1999).

From January 1996, an automated spectrophotometer installed at the Siberian Lidar Station (SLS) of IAO SB RAS has conducted regular measurements of NO_2 content in the atmosphere (NO_2 is a component of the nitrogen catalytic cycle of ozone destruction). The spectrophotometer records the spectrum of solar radiation scattered at zenith in the wavelength range 430–450 nm in the twilight period, when the solar zenith angle varies from 83° to 96°. The slant NO_2 content along the trajectory of recorded radiation is calculated from the deformation of the spectrum. Data on the slant NO_2 content in the atmosphere are used to reconstruct, through solution of the inverse problem, the vertical distribution of NO_2 in 10 layers each 5 km thick in the altitude range 0–50 km. Then the total NO_2 content is calculated as a sum over all layers. The technique of reconstruction of the NO_2 profile is borrowed from McKenzie et al. (1991).

Lidar station altitude sounding of the atmosphere (LSASA) was started in 1986. In 1988, regular observations of the vertical stratification of aerosols in the stratosphere were started. Later on they were supplemented by measurements of the vertical distributions of ozone concentrations (since 1989) and temperature (since 1995). Currently LSASA continues active investigation into the variability and disturbances of vertical profile characteristics of aerosol and temperature in the stratosphere and mesosphere.

The measurements are performed by the lidar with a receiving mirror 1 m in diameter and a transmitter at an Nd:YAG laser with a wavelength of 532 nm, pulse energy of 200 mJ, pulse repetition frequency of 10 Hz, signal accumulation time of 2 h, spatial resolution of 192 m, and signal receiving in the single-electron photopulse counting mode. The backscattered radiation was received from heights of 10–60 km (Cheremisin, Marichev, and Novikov 2011).

The aerosol scattering ratio $R(H)$ (H is current height) is used as a parameter describing the vertical stratification of aerosol. By definition, $R(H)$ is the ratio of the sum of the aerosol and molecular backscattering coefficients to molecular backscatter coefficient. For example, $R(H) = 1$ denotes the absence of aerosol at that level, and, conversely, $R(H) \geq 1$ denotes the presence of aerosol. The value of $R(H)$ is determined by the contribution of aerosol scattering in general, and, indirectly, the estimated value of the aerosol component is estimated.

Lidar measurements of vertical temperature distribution were based on the relation between molecular backscattering and atmospheric density. Temperature profiles were calculated from values of the elastic molecular (Rayleigh) scattering of a signal using the equation obtained in the assumption of validity of the ideal gas conservation equation and thermodynamic equilibrium conservation law.

Absorption spectra of the solar radiation passing through the whole atmospheric depth were recorded by the IFS–125M Fourier spectrometer. The conditions of recording were the following: spectral range of 25,000–8000 cm^{-1} (400–1250 nm), silicon photodiode as a photodetector, quartz divider, resolution of 0.05 cm^{-1}, scanner rate of 20 kHz, aperture diameter of 0.6 mm, and time for one measurement of 10 min. The spectrometer allowed measurements at an aperture diameter of 0.85 mm (the signal-to-noise ratio (*s/n*) increased 2–3-fold), but in this case convolution (distortion) of spectra in the high-frequency range (400–500 nm) was observed. In the range of 18,000 cm^{-1}, we observed $s/n = 100$. Spectra in this period were recorded from 09:00 to 18:00 LT. However, the solar radiation during the experiment was often intercepted by clouds. Therefore, the quality of the spectra was different in different periods. When the sun was fully covered by clouds, the recording was halted, because the tracking system did not allow measurements. For a detailed description, see Vasil'chenko, Serdyukov, and Sinitsa (2012).

The measurement system developed allows us to reconstruct the whole set of microphysical, chemical, and optical characteristics of aerosol from the recorded data.

3. Measuring sites

Permanent measurements of the concentration of minor constituents were carried out at the three stations for monitoring of atmospheric composition of IAO SB RAS (Figure 2): Fonovaya Observatory, TOR Station, and Basic Experimental Complex. The Fonovaya Observatory is located 60 km to the west of Tomsk, the TOR Station is situated at the northeastern end of the Tomsk Scientific Centre (Akademgorodok), and BEC lies in the suburbs 3 km to the east from Akademgorodok (Table 3). This arrangement of the stations (almost in line) in regard to the west–east transport of air mass allows us to estimate the anthropogenic contribution of the city of Tomsk to the formation of the field of atmospheric pollutants.

The vertical distribution of the climatically significant components of the troposphere was studied with the Optik Tu-134 flying laboratory. The flight started from Eltsovka airport in Novosibirsk on 22 May 2012. Immediately after takeoff, the Tu-134 aircraft started climbing to an altitude of 7000 m for the flight to the region of investigation (vicinities of Tomsk and the Fonovaya (Background) Observatory; Figure 3). Upon reaching the maximal altitude over the study region, the aircraft started a smooth descent to an altitude of 500 m above ground, step-by-step to horizontal flight (for 7 min) at eight levels: 7000, 5500, 4000, 3000, 2000, 1500, 1000, and 500 m. Then the aircraft flew to the area of the Karakanskii forest in the Novosibirsk region, where sensing by the same scheme was carried out.

The weather conditions during the flight were determined by the low-gradient, high-pressure field (Figure 4). In the regions of airborne sensing of the atmosphere, cumulus fair-weather clouds (*Cu hum*, cloud level index 4–6) were observed, and their system had a chessboard structure, thus indicating the presence of convective cells in the lower troposphere.

Temperature–wind sounding was carried out with the Vaisala R92SGP radiosonde. Table 4 shows the schedule of sounding during the experiment.

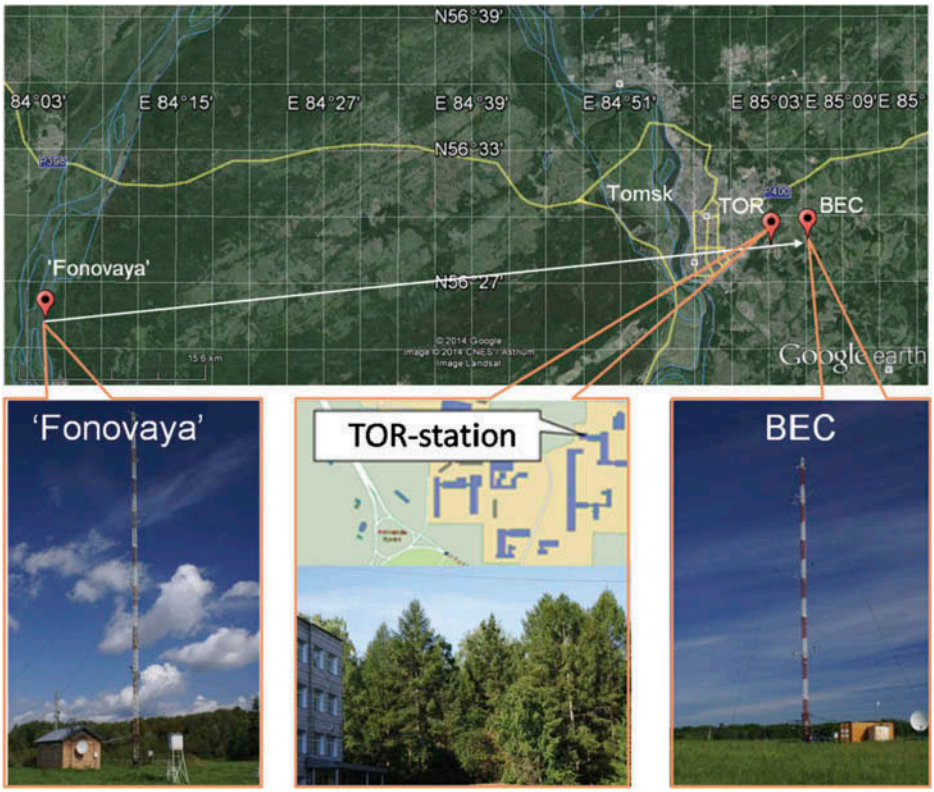

Figure 2. Arrangement of stations for atmospheric monitoring: (left) Fonovaya Observatory, (centre) TOR Station, and (right) BEC.

Table 3. Coordinates of the stations.

Station	Latitude	Longitude	Height above mean sea level (m)
TOR	56° 28′ 41″	85° 03′ 15″	133
Fonovaya	56° 25′ 07″	84° 04′ 27″	80
BEC	56° 28′ 49″	85° 06′ 08″	120

Regular monitoring of atmospheric AOT was carried out (in particular, on 22 May 2012) at the observation sites in Tomsk (IAO SB RAS) and the Fonovaya Observatory.

At the stationary Aerosol Station of IAO SB RAS located at the southeastern end of Tomsk (http://aerosol1.iao.ru; 56.5° N, 85.1° E; GMT + 7.00), characteristics of surface aerosol were monitored every hour round the clock. The Combined Aerosol Experiment on May 2012 included a cycle of simultaneous two-site measurements at the IAO Aerosol Station in Tomsk and at the mobile Aerosol Station based at the Fonovaya Observatory in the forest zone 70 km to the west of Tomsk. Mass concentrations of aerosol and black carbon were measured every hour round the clock on 17–24 May at the two measurement sites.

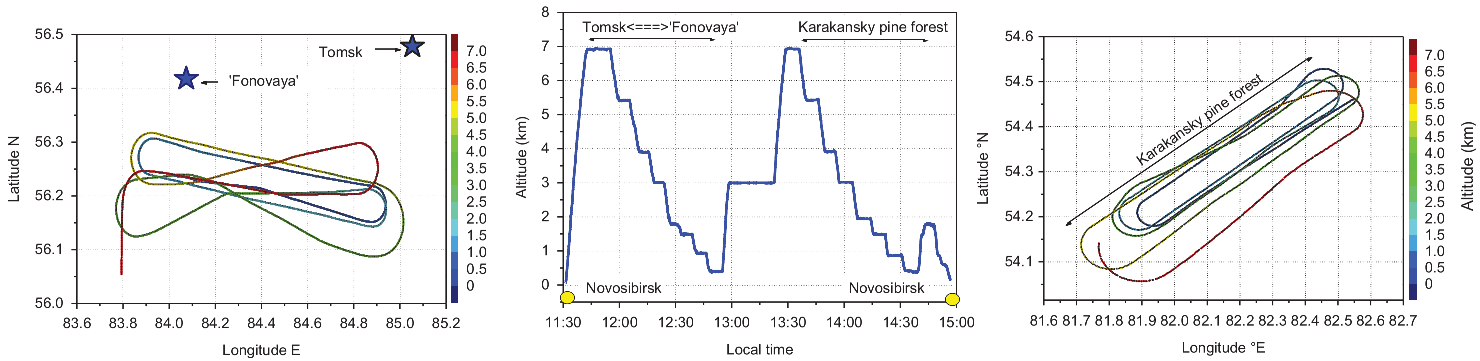

Figure 3. Flight scheme: horizontal structure of flights over the study regions (left and right); temporal diagram of flight altitudes (centre).

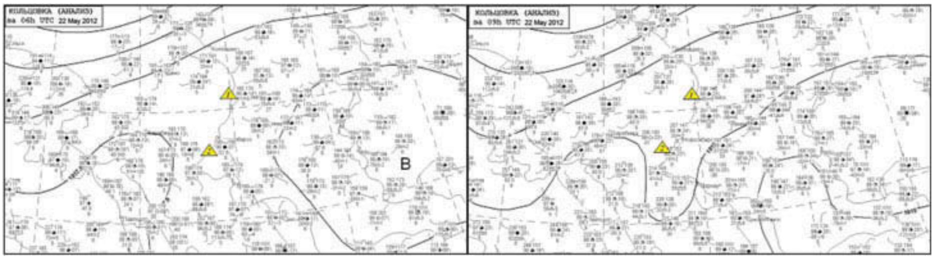

Figure 4. Fragments of ring weather maps for 06.00 and 09.00 GMT on 22 May 2012. Yellow triangles denote the regions of vertical sensing of the atmosphere: 1 – Tomsk–Fonovaya, 2 – Karakanskii forest.

Table 4. Schedule of radio sounding.

Date	Local time	Parameters	Maximal height (km)
23 May 2012	01:00	*t*, *U*,wind speed, and direction	26
23 May 2012	19:10		24
25 May 2012	13:00		25
25 May 2012	19:00		25
26 May 2012	07:20		23
26 May 2012	13:00		24
26 May 2012	19:00		25
27 May 2012	01:00		25

Aerosol fields of the vertical depth of the troposphere were sensed with the aid of the LOZA-S stationary multifrequency lidar. The sensing on 22–23 May 2012 was conducted continuously from 06:00 local time on 22 May to 20:00 local time on 23 May.

On 14–27 May 2012, the two-site radiative experiment was conducted in Tomsk and at the Fonovaya Observatory. This experiment invoked the data of the MODIS multichannel spectroradiometer installed on Terra and Aqua platforms of the EOS satellite system.

Within the framework of the Combined Radiative Experiment (14–27 May 2012), the acoustic diagnostics of the atmospheric boundary layer were carried out with the use of local and remote facilities. Local facilities – Metec-2 Ultrasonic Meteostations (USMs) – were installed at the territory of the Fonovaya Observatory IAO SB RAS (Kireevsk) and in Tomsk on the roof of the laboratory building of IAO SB RAS. Meteo-2 USMs operated round the clock in permanent mode to measure mean values and turbulent characteristics of wind and air temperature, as well as static atmospheric pressure and relative air humidity. The sodar operated every day from 08:00 to 21:00 LT. The main purpose of this device was to measure the height of the layer of intense turbulent heat exchange and components of the wind vector in this layer (height range 50–700 m).

At the IAO SLS located in Tomsk (56.5° N, 85.0° E), the automated spectrophotometer measured the nitrogen dioxide content in the atmosphere during morning and evening twilight on 14–27 May 2012.

In addition, absorption spectra of solar radiation passing through the entire atmospheric depth were recorded by the IFS–125M Fourier spectrometer in the period 17–23 May 2012.

At the LSASA, 12 separate night soundings of the stratosphere were conducted in May of 2012, including the night of 22 May.

Thus, during the Combined Experiment in May 2012, the entire set of microphysical, chemical, and optical characteristics of aerosol in Southwestern Siberia was studied simultaneously with the unique measurement system including ground-based, airborne, and spaceborne measurement facilities.

4. Results of Combined Aerosol Experiment

In the Combined Aerosol Experiment, continuous synchronous measurements of the concentrations of minor atmospheric constituents were conducted. As an example, we demonstrate the time diagrams of variation in aerosol particle number density and CO_2 concentration at the three ground–based monitoring stations (see Table 3). The results of these measurements from the period 17–24 May 2012 are shown in Figure 5.

It will be seen from Figure 5 that over the period of the experiment, the photosynthetic activity of Siberian land ecosystems was low, since the carbon dioxide concentration observed at all three stations was at a high level, even in daytime. The diurnal dynamics of both aerosol and CO_2 concentrations was mostly determined by the dynamics of the mixing layer, that is, in daytime the development of vertical air flows due to the heating of the surface led to a decrease in concentration due to dilution, while at night, with development of temperature inversion, atmospheric admixtures accumulated in the thin atmospheric surface layer.

To study the vertical distribution of the main greenhouse gases we used the analytical instrumentation installed on board the Optik Tu-134 Flying Laboratory. This instrumentation included the precision Picarro G2301-m gas analyser, which allows CO_2, CH_4, and H_2O concentrations to be measured with accuracy: <200 ppb, <1.5 ppb, and <150 ppm, respectively. The Picarro gas analyser was used to study the vertical distribution of CO_2, CH_4, and H_2O concentrations during the Tomsk–Fonovaya flight (22 May 2012). An example of the vertical profiles obtained is shown in Figure 6.

A distinctive feature of the CO_2 concentration profile measured near the city of Tomsk and the Fonovaya Observatory is a decrease in the CO_2 content in the layer between 3.5 and 4.5 km. The median value of the CO_2 concentration in the troposphere over the region was 397.7 ppm (lower quartile $x_{0.25}$ = 397.3; higher quartile $x_{0.75}$ = 398.2).

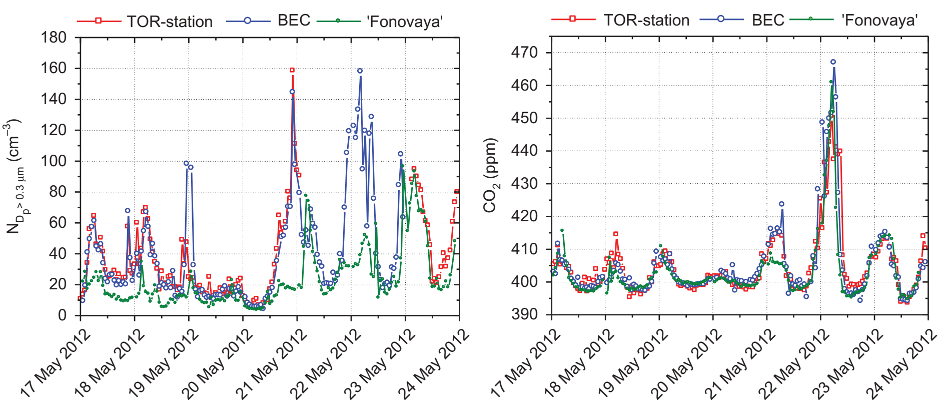

Figure 5. Time profiles of total aerosol particle number density in the range 0.3 μm < Dp < 20 μm ($N_{Dp\ >\ 0.3\ \mu m}$) and the CO_2 concentration as measured at the three monitoring stations during the Combined Experiment.

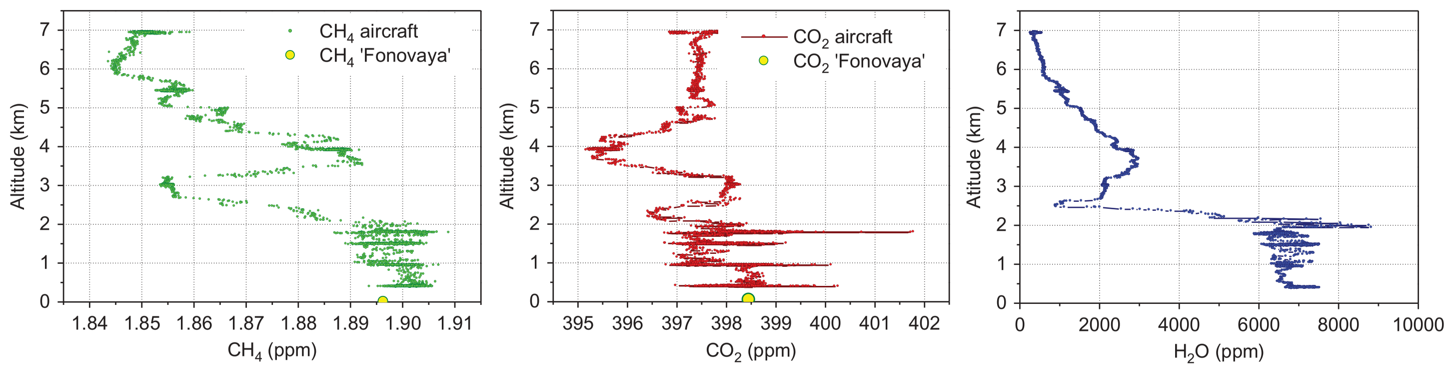

Figure 6. Vertical distribution of CO_2, CH_4, and H_2O concentrations for Tomsk–Fonovaya Flight (22 May 2012).

A characteristic feature of the vertical methane distribution was the practically uniform distribution of CH_4 in the atmospheric layer from the Earth's surface to a height of 2–2.2 km due to the vertical mixing developed. Above the boundary of the mixing layer, the CH_4 concentration began to decrease sharply. In the free troposphere, the layered structure of methane distribution appeared. This structure was likely caused by the long-range transport of raw biomass burning plumes from remote regions, since in the case of local fires such layers should also appear within the increased content of CO_2.

Results of temperature–wind sensing with the Vaisala R92SGP radiosonde launched at 19:10 local time on 23 May 2012 are shown in Figure 7. The troposphere mostly showed potentially stable stratification except for a layer with potentially unstable stratification between 750 and 680 hPa. The vertical gradient of air temperature γ in the troposphere was ≈ –0.77°C/100 m. The tropopause height (t = –61.45°C) was 11 km asl. Near the tropopause, the radiosonde crossed the jet flow, in which the wind velocity reached 28.2 m s^{-1}.

Figure 8 illustrates the temporal profile of spectral AOT and *W*, the total atmospheric water content measured on 22 May 2012, by sun photometers in Tomsk (IAO SB RAS) and at the Fonovaya (Background) Observatory. The value of the total water content of the atmosphere and the diurnal dynamics in these two regions are close to average multi-year values for this period. The AOT profile differs from the average diurnal profile, and these differences are more pronounced in Tomsk. In contrast to the increase in aerosol turbidity till ~17:00 LT and the later decrease, on 22 May 2012 we observed a decrease to midday, and then AOT stabilized near to average values for May.

During the Combined Aerosol Experiment, the instrumental system (Shmargunov et al. 2008; Shmargunov and Pol'kin 2007; Kozlov, Shmargunov, and Pol'kin 2008) was used to conduct simultaneous measurements of the concentrations of submicron aerosol and black carbon at Tomsk (Kozlov et al. 1997) and Fonovaya Observatory. Figure 9 illustrates the time profiles of aerosol and black carbon (BC) concentrations (a) and the dynamics of the single scattering albedo of the dry aerosol fraction and the parameter of condensation activity of particles (b).

The time profiles of the aerosol and BC concentrations are close in shape and characterized by synchronous variations at the two measurement sites. The concentration values in the period of 17–19 May are close to the background spring level, and at the second stage of the experiment they increased for aerosol and BC to 50 and 3 μg m^{-3}, respectively (Figure 9(*a*)). Concentration variations led to the situation where the relative BC content of particles increased at the final stage of observations, thus leading to a decrease in single scattering albedo, on average, from 0.96 to 0.87–0.90 (Figure 9(*b*)). The time dynamics of aerosol characteristics is accompanied by gradual decrease in the parameter of condensation activity of particles γ, which characterizes the increase in the aerosol scattering coefficient at increasing relative air humidity.

In May–June, within the framework of the Combined Aerosol Experiment, we conducted the sensing of the vertical structure of aerosol fields in the troposphere with the aid of the stationary LOZA multifrequency lidar. As an example, Figure 10 shows a fragment of the space–time profile of the tropospheric aerosol field in units of the scattering ratio (ratio of the sum of aerosol and molecular scattering to the molecular) for 22–23 May 2012. This fragment illustrates the typical diurnal behaviour of the aerosol structure. It will be seen that as the surface becomes warmer and the temperature of the surface layer increases (from 7°C in the morning to 17°C in the daytime), upwelling flows appear, and the height of the mixing layer increases rapidly and by 12:00 LT reaches the height of the atmospheric boundary layer (2.2 km), at which point the rising humid air condenses and some cumulus clouds are formed. By the night of 23 May, we observed the gradual

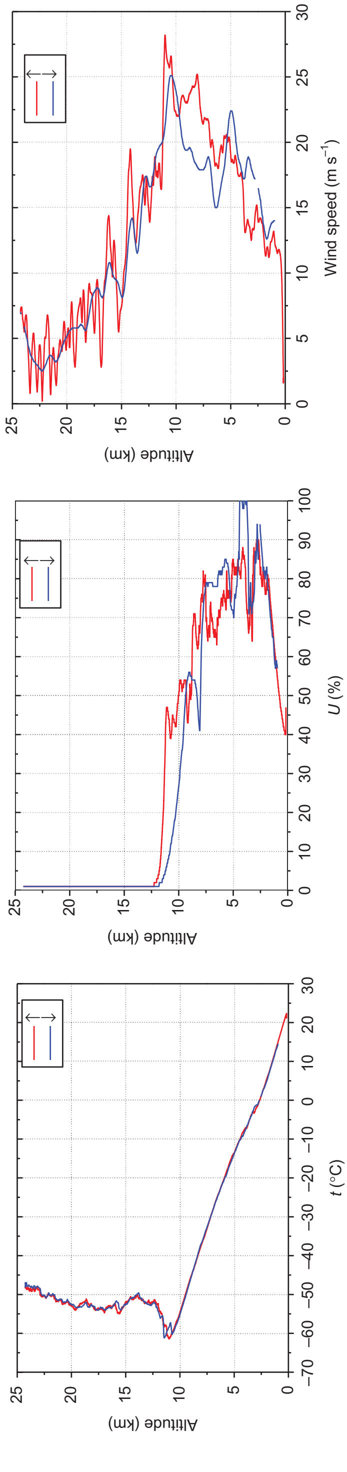

Figure 7. Vertical profiles of temperature, relative humidity, and wind velocity obtained at the time of radiosonde launching at 19:10 LT on 23 May 2012.

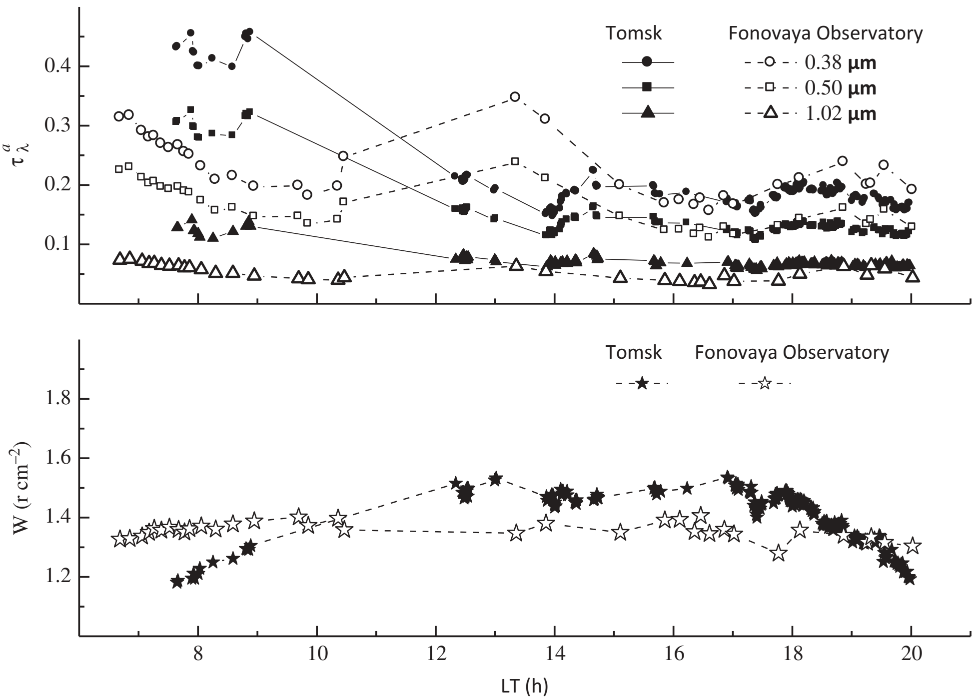

Figure 8. Variations in spectral AOT (0.38, 0.5, 1.02 μm) and atmospheric total water on 22 May 2012 in the two monitoring regions (r is the mixing ratio of (water vapour plus droplets) and dry air).

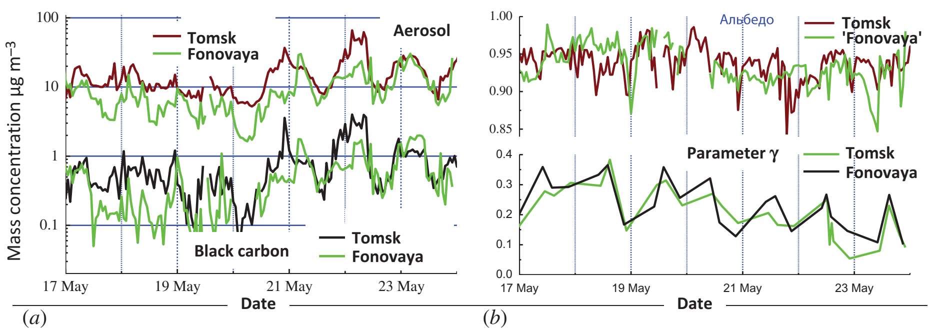

Figure 9. Time profiles of the radiation-significant parameters of aerosol and black carbon at the IAO Aerosol Station (Tomsk) and the Fonovaya Observatory during the Combined Experiment: (a) concentrations of aerosol and black carbon; (b) single scattering albedo ω of the dry particulate fraction at a wavelength of 0.51 μm and the parameter of condensation activity of particles γ.

descent of both the height of the boundary layer and the overlying aerosol layers due to the approach of a low-pressure zone.

As a result of satellite monitoring, for the period of the Combined Experiment we obtained a vast amount of information for Tomsk and Kireevsk on the following environmental parameters:

- spectral aerosol optical thickness (λ = 0.47, 0.55, 0.66, 2.1 μm);

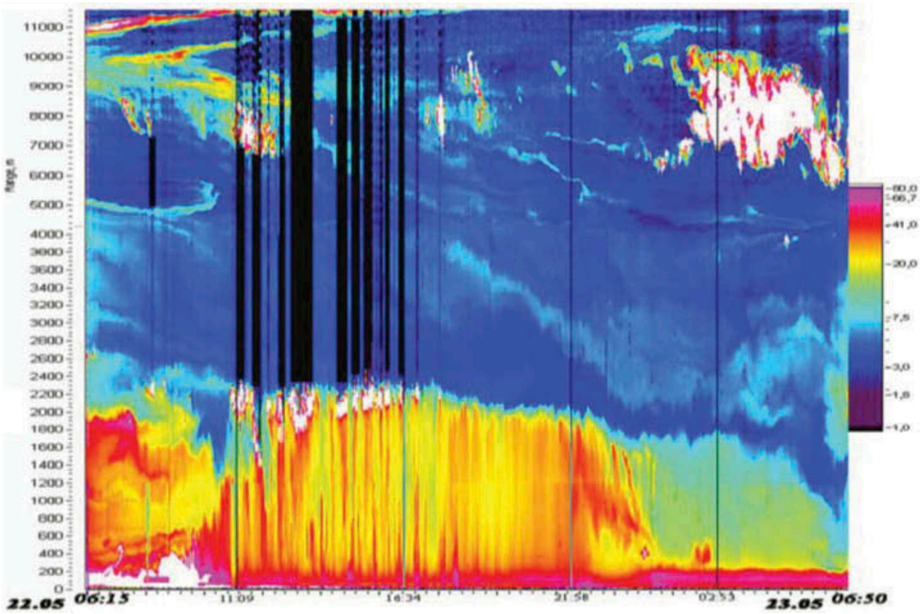

Figure 10. Space–time profile of the tropospheric aerosol field in units of the scattering ratio as judged from the LOZA-S lidar data from 06:15 LT on 22 May 2012 to 06:50 LT on 23 May.

- cloud parameters, namely, pressure and temperature of the cloud top, its moisture content, optical thickness, effective radius of particles, cirrus cloud amount;
- vertical profiles of temperature, humidity, and ozone, as well as integral content of water vapour and ozone in the atmosphere;
- air temperature T_A and dew point T_D at altitudes from 8 to 12 km (layer of 300–200 mb);
- profiles and integral content of some minor atmospheric constituents in the atmosphere: sulphur dioxide (SO_2), nitrogen dioxide (NO_2), ozone (O_3), carbon monoxide/dioxide (CO/CO_2), methane (CH_4).

The values of T_A and T_D at altitudes of 8–12 km characterized the temperature–humidity conditions in the atmospheric layer in which the cirrus clouds were observed. The satellite information obtained served for a thorough description of the status of the atmosphere at different periods of the experiment, including 22 May.

As a result of the operation of acoustic facilities, we compiled a database including estimates of 22 turbulence parameters (first and second moments of wind velocity components and air temperature) in the surface atmospheric layer at the two observation sites (Tomsk and Fonovaya Observatory), as well as vertical profiles of wind speed and direction in Tomsk. The archive of initial experimental data available provides the possibility of extending the list of reconstructed meteorological parameters.

As an example of the operation of acoustic facilities on 22 May 2012, Figure 11 demonstrates the diurnal profile of the vertical turbulent flux of heat and kinetic energy of turbulence in the atmospheric surface layer (measurements by Meteo-2 ultrasonic meteorological stations), as well as the speed of the vertical component of the wind vector at altitudes of 60 and 140 m (Volna sodar). The estimates were obtained from 10 min time intervals.

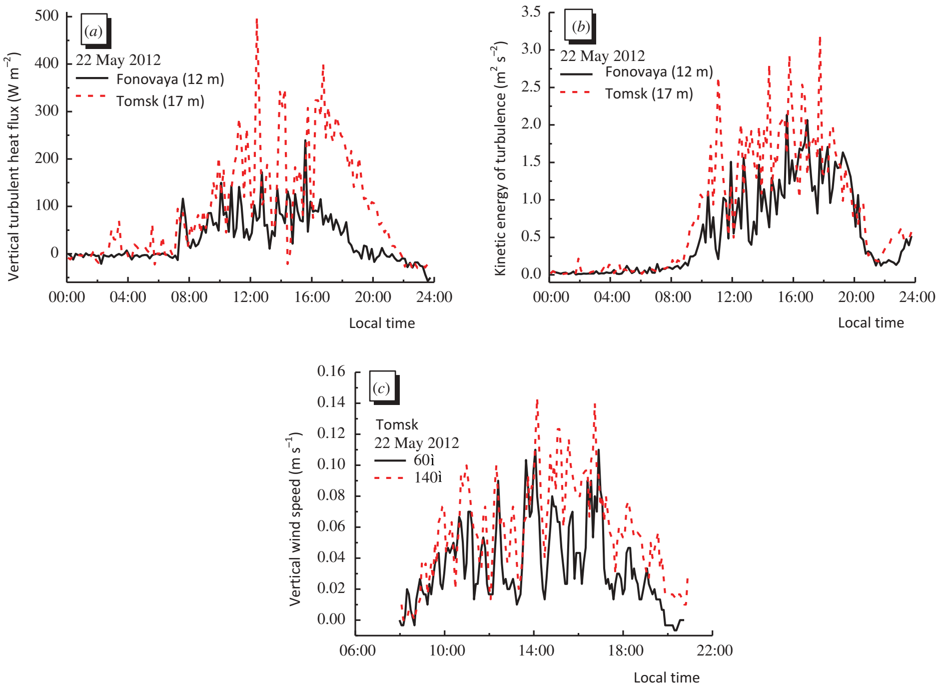

Figure 11. Examples of measurement of meteorological characteristics by acoustic facilities: (*a*) vertical turbulent heat flux; (*b*) kinetic energy of turbulence; (*c*) vertical wind speed at two heights. Estimates are obtained from 10-min measurement intervals.

The examples shown in Figure 11 are characteristic of this measurement season, having typical diurnal behaviour and demonstrating the difference between turbulence characteristics under conditions of natural landscape (Fonovaya Observatory) and over urban territory (Tomsk): turbulent heat flux and the kinetic energy of turbulence are much higher over urban territory as compared with the natural landscape. The 10-min averaged vertical component of the wind vector at a height of 140 m is somewhat higher than that at a height of 60 m. The positive sign of vertical velocity and relatively high daytime values indicate the presence of strong convective flows favouring aerosol transport from the surface layer to higher atmospheric layers.

Within the framework of the Combined Experiment, the atmospheric content of NO_2 was measured in the period 14–27 May 2012, during morning and evening twilight. Figure 12 shows the profiles of NO_2 content in the atmospheric column for the evening measurements. The analysis of these profiles shows that the maximal value of NO_2 content is in the layer at 30–35 km. This is 5 km higher than the statistically average profile for this season. The values at the maxima correspond to statistically average values, except for 21 and 24 May. On these two days, the values of the maxima were two to three times lower than the average. Also to be noted are the 20 and 27 May, when the NO_2 content in the troposphere was high due to either unstable weather conditions or transport of air masses polluted by NO_2 of industrial origin.

The results of measurement of vertical aerosol stratification for the last ten days of month are shown in Figure 13. One can see that on the night of 22 May the atmosphere was almost free of aerosol. This situation is typical of the warm season. The monitoring of

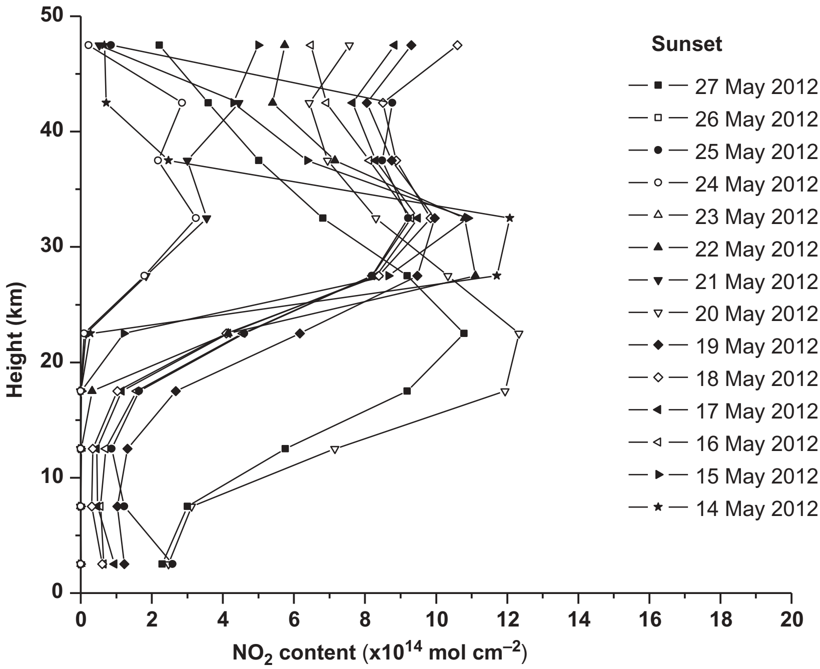

Figure 12. Profiles of NO_2 [$\times 10^{14}$ mol cm^{-2}] content in the atmospheric column.

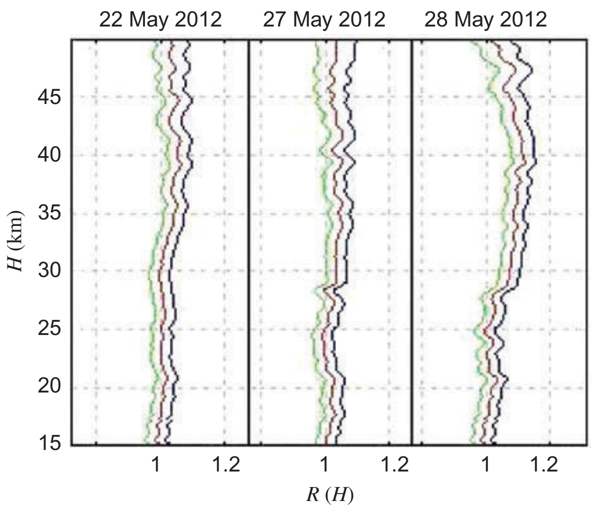

Figure 13. Vertical structure of aerosol over Tomsk: profiles of aerosol scattering ratio and its standard deviation.

vertical temperature distribution is shown in Figure 14. The lidar temperature profile is close to the model and that measured from Aura, which is also typical for summertime.

Absorption spectra of solar radiation passing through the Earth's atmosphere were recorded by the IFS-125M Fourier spectrometer.

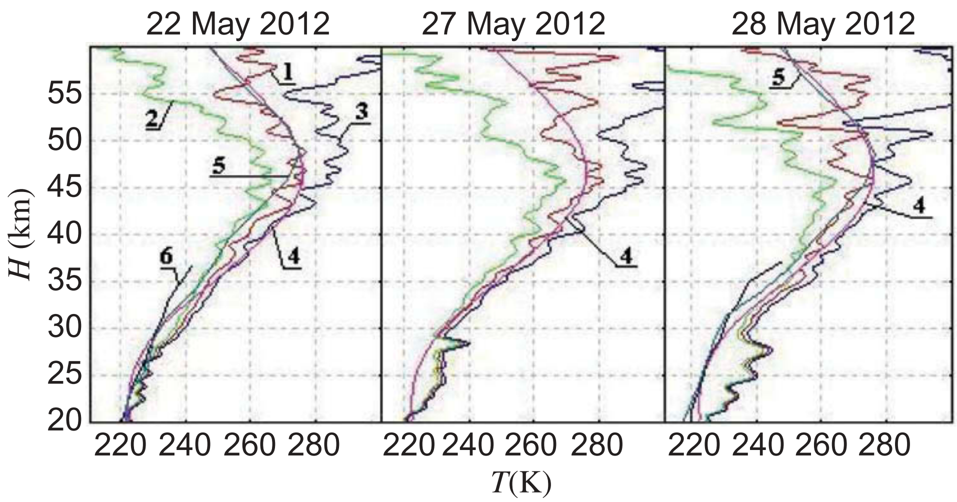

Figure 14. Vertical distribution of temperature over Tomsk: (1) lidar profiles; (2 and 3) range of standard deviation; (4, 5, and 6) temperature profiles of the CIRA-86 model, measurements from Aura and by radiosonde.

A typical recorded spectrum is shown in Figure 15. The results were processed by SFIT v3.92. As a result of processing of the experimental data, we have reconstructed the total content of water vapour with the use of a spectral range 9900–10,000 cm^{-1}.

The more detailed description of the total content of water vapour and determination of profiles, as well as a description of correlations, can be found in Makarova et al. (2014). In addition, using the original technique (Vasilchenko et al. 2012) we obtained the

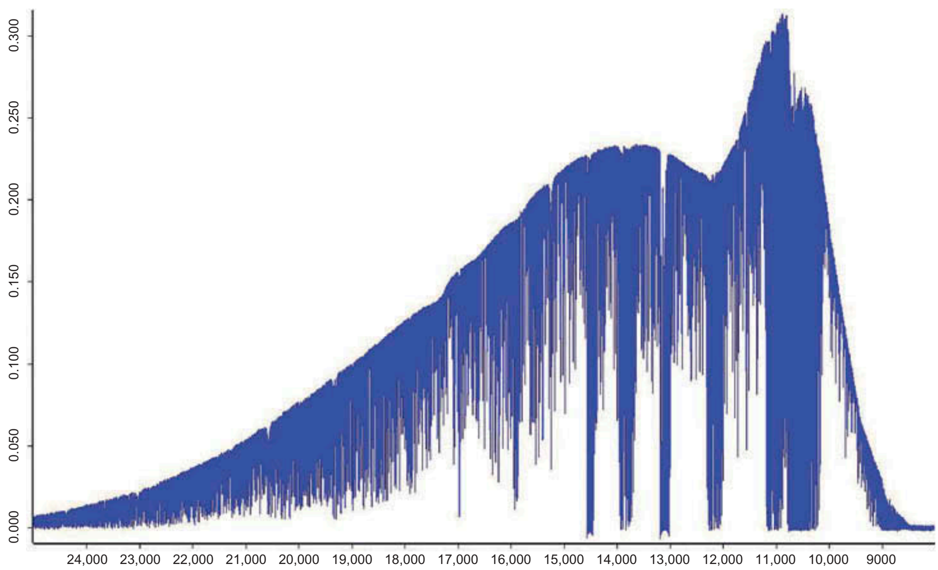

Figure 15. Absorption spectrum of solar radiation on 22 May 2012, in the range 8000–25,000 cm^{-1}.

total content of ozone and oxygen dimers $(O_2)_2$ as a result of analysis of solar radiation spectra in the range 15,000–18,000 cm^{-1}.

5. Conclusions

The development of this unique measurement system has allowed us to conduct simultaneous measurements of microphysical, chemical, and optical properties of aerosol particles in the surface layer and in the free atmosphere with the use of various ground-based, airborne, and spaceborne facilities in order to elucidate the complete pattern of the composition and status of the atmosphere in the territory of Southwestern Siberia

The Combined Experiment on measurement of various atmospheric parameters in the Siberian region in May 2012 has become a first step on the way of joining the efforts of different research groups aimed at obtaining information as complete as possible about the status of the atmosphere under conditions of changing climate. Despite the short duration of the experiment, it has demonstrated the potential capabilities of measuring facilities available for longer-term measurements in the future. In addition, the measurements have revealed some disadvantages. In particular, it was shown that the capabilities of many ground-based and spaceborne devices for active and passive sensing of the atmosphere are severely limited by the presence of dense clouds. According to multi-year observations, only 38 cloudless days per year are observed on average in Tomsk. In this respect airborne sensing has an advantage, but the use of the flying laboratory remains limited due to its high cost. Thus, the conducting of continuous combined observations now seems possible only in the atmospheric boundary layer.

Nevertheless, the data obtained during the Combined Experiment are of great value for validation, correction, and calibration of satellite measurements and for validation and improvement of climatic models.

Funding

This work was supported, in part, by Programme no. 4 of Presidium RAS; Programme no. 5 of Division of Earth Sciences RAS; SB RAS Interdisciplinary Integration Projects nos 8, 31, 35, 70, and 131; RFBR Grants Nos. [11–05–93118], [12–05–00395], [13–05–00096], [13–08–98013], [13–05–98074], [14–05–00526], [14–05–00590], and [14–05–92003]; Grant of the President of RF in Support of Leading Scientific Schools, NSh–4714.2014.5; Ministry of Science and Education of the RF [no. 14.604.21.0046] and [no. 14.604.21.0100]; and the Russian Science Foundation [no. 14-27-00022].

References

Anokhin, G. G., P. N. Antokhin, M. Y. Arshinov, V. E. Barsuk, B. D. Belan, S. B. Belan, D. K. Davydov, G. A. Ivlev, A. V. Kozlov, V. S. Kozlov, M. V. Morozov, M. V. Panchenko, I. E. Penner, D. A. Pestunov, G. P. Sikov, D. V. Simonenkov, D. S. Sinitsyn, G. N. Tolmachev, D. V. Filipov, A. V. Fofonov, D. G. Chernov, V. S. Shamanaev, and V. P. Shmargunov. 2011. "OPTIK Tu–134 Aircraft Laboratory." *Atmospheric and Oceanic Optics* 24: 805–816.

Arshinov, M. Y., B. D. Belan, D. K. Davydov, G. A. Ivlev, A. V. Kozlov, D. A. Pestunov, E. V. Pokrovskii, G. N. Tolmachev, and A. V. Fofonov. 2007. "Sites for Monitoring of Greenhouse Gases and Gases Oxidizing the Atmosphere." *Atmospheric and Oceanic Optics* 20: 45–53.

Cheremisin, A. A., V. N. Marichev, and P. V. Novikov. 2011. "Lidar Observations of Volcanic Aerosol Content in the Atmosphere over Tomsk." *Russian Meteorology and Hydrology* 36 (9): 600–607. doi:10.3103/S1068373911090056.

Dubovik, O., B. Holben, Y. Kaufman, M. Yamasoe, A. Smirnov, D. Tanré, and I. Slutsker. 1998. "Single–Scattering Albedo of Smoke Retrieved from the Sky Radiance and Solar Transmittance Measured from Ground." *Journal of Geophysical Research* 103 (D24): 31903–31923. doi:10.1029/98JD02276.

Dubovik, O., A. Smirnov, B. Holben, M. King, Y. Kaufman, T. Eck, and I. Slutsker. 2000. "Accuracy Assessments of Aerosol Optical Properties Retrieved from Aerosol Robotic Network (AERONET) Sun and Sky Radiance Measurements." *Journal of Geophysical Research* 105 (D8): 9791–9806. doi:10.1029/2000JD900040.

Dubovik, O. T., and M. King. 2000. "A Flexible Inversion Algorithm for Retrieval of Aerosol Optical Properties from Sun and Sky Radiance Measurements." *Journal of Geophysical Research* 105 (D16): 20673–20696. doi:10.1029/2000JD900282.

Eremenko, S., and A. Ankilov. 1995. "Conversion of the Diffusion Battery Data to Particle Size Distribution: Multiple Solutions Averaging Algorithm (MSA)." *Journal of Aerosol Science* 26 (Suppl 1): S749–S750. doi:10.1016/0021-8502(95)97282-J.

Gladkikh, V. A., A. P. Kamardin, and I. V. Nevzorova. 2009. "Determination of Internal Mixing Layer Height from "Volna" Sodar Measurements." *Atmospheric and Oceanic Optics* 22: 1154–1159.

Gladkikh, V. A., and A. E. Makienko. 2009. "Digital Ultrasonic Meteostation." *Pribory* 7 (109): 21–25.

Gladkikh, V. A., A. E. Makienko, and V. A. Fedorov. 1999. "Volna–3 Doppler Sodar." *Atmospheric and Oceanic Optics* 12: 422–429.

Holben, B. N., T. F. Eck, I. Slutsker, D. Tanré, J. P. Buis, A. Setzer, E. Vermote, J. A. Reagan, Y. J. Kaufman, T. Nakajima, F. Lavenu, I. Jankowiak, and A. Smirnov. 1998. "AERONET – A Federated Instrument Network and Data Archive for Aerosol Characterization." *Remote Sensing of Environment* 66: 1–16. doi:10.1016/S0034-4257(98)00031-5.

Kozlov, V. S., A. G. Panchenko, S. A. Terpugova, V. V. Pol'kin, and E. P. Yausheva. 2002. "Dynamics of Temporal Variability in Characteristics of Near–Surface Submicron Aerosol and Black Carbon in Western Siberia." In *Big Vasyugan Bog. Current State and Development Processes*, edited by M. V. Kabanov, 156–164. Tomsk: IAO SB RAS.

Kozlov, V. S., M. V. Panchenko, A. G. Tumakov, V. P. Shmargunov, and E. P. Yausheva. 1997. "Some Peculiarities of the Mutual Variability of the Content of Soot and Submicron Aerosol in the Near– Ground Air Layer." *Journal of Aerosol Science* 28: SS231–SS232. doi:10.1016/S0021-8502(97)85116-6.

Kozlov, V. S., M. V. Panchenko, and E. Yausheva. 2008. "Mass Fraction of Black Carbon in Submicron Aerosol as an Indicator of Influence of Smoke from Remote Forest Fires in Siberia." *Atmospheric Environment* 42: 2611–2620. doi:10.1016/j.atmosenv.2007.07.036.

Kozlov, V. S., V. P. Shmargunov, and V. V. Pol'kin. 2008. "Spectrophotometers for Investigation of Characteristics of Radiation Absorption by Aerosol Particles." *Pribory i Tekhnika Eksperimenta* 155–157.

Makarova, M. V., V. I. Serdyukov, M. Y. Arshinov, B. A. Voronin, B. D. Belan, L. N. Sinitsa, E. R. Polovtseva, S. S. Vasilchenko, and D. M. Kabanov. 2014. "First results of ground-based Fourier Transform Infrared (FTIR) measurements of the H_2O total column in the atmosphere over West Siberia." *IJRS* 15: 5637–5650. doi:10.1080/01431161.2014.945016.

Marenco, A., V. Thouret, P. Nédélec, H. Smit, M. Helten, D. Kley, F. Karcher, P. Simon, K. Law, J. Pyle, G. Poschmann, R. Von Wrede, C. Hume, and T. Cook. 1998. "Measurement of Ozone and Water Vapor by Airbus In-Service Aircraft: The MOZAIC Airborne Program, an Overview." *Journal of Geophysical Research* 103 (D19): 25631–25642. doi:10.1029/98JD00977.

McKenzie, R. L., P. V. Johnston, C. T. McElroy, J. B. Kerr, and S. Solomon. 1991. "Altitude Distributions of Stratospheric Constituents from Ground-Based Measurements at Twilight." *Journal of Geophysical Research* 96 (D8): 15499–15511. doi:10.1029/91JD01361.

Monnin, E., A. Indermuhle, A. Dallenbach, J. Fluckinger, B. Stauffer, T. F. Stocker, D. Raynaud, and J.-M. Barnola. 2001. "Atmospheric CO_2 Concentrations over the Last Glacial Termination." *Science* 291: 112–114. doi:10.1126/science.291.5501.112.

Odintsov, S. L., and V. A. Fedorov. 2007. "Investigation of Wind Velocity Variations on Mesometeorological Scale from Sodar Observations." *Atmospheric and Oceanic Optics* 20: 900–906.

Sakerin, S. M., D. M. Kabanov, A. P. Rostov, S. A. Turchinovich, and V. V. Knyazev. 2012. "Sun Photometers for Measuring the Spectral Atmospheric Transparency under Stationary and Mobile Conditions." *Atmospheric and Oceanic Optics* 25: 1112–1117.

Sakerin, S. M., D. M. Kabanov, A. P. Rostov, S. A. Turchinovich, and Y. S. Turchinovich. 2004. "System for the Network Monitoring of the Atmospheric Constituents Active in Radiative Processes. Part 1. Sun Photometers." *Atmospheric and Oceanic Optics* 17: 314–320.

Samoilova, S. V., Y. S. Balin, G. P. Kokhanenko, and I. E. Penner. 2009. "Investigations of the Vertical Distribution of Troposphere Aerosol Layers Based on the Data of Multifrequency Raman Lidar Sensing: Part 1. Methods of Optical Parameter Retrieval." *Atmospheric and Oceanic Optics* 22: 302–315. doi:10.1134/S1024856009030075.

Shmargunov, V. P., V. S. Kozlov, A. G. Tumakov, V. V. Pol'kin, and M. V. Panchenko. 2008. "FAN-Based Automated Aerosol Nephelometer." *Pribory i Tekhnika Eksperimenta* (p): 165.

Shmargunov, V. P., and V. V. Pol'kin. 2007. "AZ-5 Based Aerosol Counter." *Pribory i Tekhnika Eksperimenta* (2): 165.

Shmargunov, V. P., V. V. Pol'kin, A. G. Tumakov, M. V. Panchenko, and V. Pol'kin Vas. 2010. "Closed-Volume Aureole Photometer." *Pribory i Tekhnika Eksperimenta* (6): 155–157.

Solomon, S., D. Qin, M. Manning, Z. Chen, M. Marquis, K. B. Averyt, M. Tignor, and H. L. Miller, eds. 2007. *Climate Change 2007: The Physical Science Basis, Contribution of Working Group I to the Fourth Assessment Report of the Intergovernmental Panel on Climate Change*. Cambridge: Cambridge University Press. IPCC AR4 WG1. ISBN978–0–521–88009–1.

Vasil'chenko, S. S., V. I. Serdyukov, and L. N. Sinitsa. 2012. "Spectral System with Optical Fiber Tracking System for Gaseous Atmospheric Component Measurement and Some Results of Spectra Analysis." *Atmospheric and Oceanic Optics* 25: 920–925.

Vasilchenko, S. S., B. A. Voronin, L. N. Sinitsa, V. I. Serdyukov, and E. R. Polovtseva. 2012. "Ground-Based Spectroscopic Measurements of Atmospheric Oxygen Complexes $(O_2)_2$." *Eighteenth International Symposium on Atmospheric and Ocean Optics: Atmospheric Physics* 8696: 869603–869607. doi:10.1117/12.2008450.